Photo-Claisen Rearrangement of Allyl Phenyl Ether in Microflow: Influence of Phenyl Core Substituents and Vision on Orthogonality

Elnaz Shahbazali[1], Timothy Noël[1] and Volker Hessel[1]

[1]*Department of Chemical Engineering and Chemistry, Micro Flow Chemistry and Process Technology, Eindhoven University of Technology, Eindhoven 5600 MB, The Netherlands*

Received: 29 June 2016; accepted: 22 August 2016

We converted diverse commercial meta-substituted phenols to the allyl-substituted precursors via nucleophilic substitution using batch technology to allow processing these in microflow by means of the photo-Claisen rearrangement. The latter process is researched on its own, as detailed below, and also prepares the ground for a fully continuous two-step microflow synthesis, as outlined above. It is known that batch processing of electronically deactivated phenols (e.g., bearing a cyano or nitro group) has several orders of magnitude lower reactivity than their parental counterparts [1]. Thus, we here explore if the high quantum yield of microflow, yet at very short residence time, is sufficient to activate the deactivated molecules. In addition, the realization of a true orthogonal two-step flow synthesis can open the door to a large synthetic scope of our approach and possibly overcome limitations due to missing orthogonality of our previously reported thermal approach of combined nucleophilic substitution-Claisen rearrangement in microflow. Consequently, we make for our photo microflow approach an orthogonality check, as previously reported for the thermal approach, and compare both.

To get a broader picture, we have investigated some major parametric sensitivities such as the irradiation intensity, the choice of solvent, the reactant concentration, and, most notably, the influence of the substitution pattern. The irradiation intensity was varied by increasing distance between a lamp and the microflow capillary. In addition, the normal photo-Claisen microflow process (at room temperature) is compared to a high-temperature photo-Claisen microflow process, to check the potential of such novel process window [2]. This is difficult to realize in batch, as the combination of strong ultraviolet (UV) irradiation and high temperature causes a high hazard potential. Yet, under microflow, this can be safely handled.

Keywords: flow chemistry, microreactors, photo-Claisen rearrangement, microreactor networks, flow orthogonality

1. Introduction

The Claisen rearrangement, which is the [3,3]-sigmatropic rearrangement of allyl phenyl ethers, makes a valuable synthetic transformation for organic chemistry [3–5]. The thermal Claisen rearrangement requires high temperatures in order to result in sufficient conversion.

In the last decade, microreactor technology has revealed promising potential for many synthetic applications and has even been applied on an industrial scale [6, 7]. Microreactor technology has also been proven beneficial for the Claisen rearrangement [8–11].

Recently, we reported on the combination of a nucleophilic substitution to the thermal-Claisen rearrangement in microflow, i.e., a continuous microflow two-step synthesis [12]. In the first step thereof, phenol and allyl bromide yield phenyl allyl ether which is then in a second step and directly converted by the thermal Claisen rearrangement. Targeting synthetic scope, the motivation was to show that, in this way, many substituted phenyl allyl ethers may derive from respectively substituted phenols. Yet, as reported, just combining the individual microflow syntheses was by no means sufficient, which is surprising. Rather, both syntheses lacked considerably in orthogonality. This was partly due to the remaining base 1,8-diazabicyclo [5.4.0]undec-7-en (DBU), which acts as catalyst for the allyl group substitution, and caused cleavage of the Claisen products to the phenol starting material. Unexpected was that the allyl bromide had similar strong effect. Under the high temperatures used in the thermal Claisen rearrangement, which are typically set in microflow even higher [13, 14], the allyl bromide decomposes to give propene and HBr. The latter acid can lead to the same decomposition rate of the Claisen product as the acid does. As a consequence, we have discussed several continuous acid or base removal techniques based on extraction and adsorption. We discussed all the advantages and disadvantages. Finally, the preference was given to using Amberlyst A21 and A26 ion exchanger in a packed bed configuration. Yet, we also noted a mismatch in the capacities of the synthesis and the purification, which led to an unacceptable mismatch in the dimensions (inner diameter) of the reaction capillary and the packed-bed tube. The latter was much too low. Therefore, we proposed a much faster exchange of packed-bed columns than common with these materials to provide fresh ion exchanger material with shorter cycle. In this way, the dimensional fit between reaction capillary and adsorption packed was smaller, although still far from being ideal. The latter would finally ask for a better ion exchange material with, e.g., much higher packing density.

Microreactors have also received a lot of attention in photochemical applications since they are capable of improving some issues related to the batch photochemistry [15, 16]. In essence, the narrowness of the microreactor channels enables a better exposure of the reaction mixture to the irradiated light and modern light-emitting diode (LED) technology avoids the unwanted warming up of the reaction solutions. A greater amount of reactant molecules is excited under more defined experimental protocol, and thus, the reaction is expedited.

As mentioned above, for the thermal-Claisen rearrangement, the photo-Claisen rearrangement can be connected similarly to a nucleophilic substitution, which introduces the allyl group into diverse phenols. Here, the main advantage is the possibility to generate para-substituted products besides the ortho-substitution pattern (for details on mechanism of photo-Claisen rearrangement, one is referred to refs. [17–20]). Yet, it should be noted as well that this generates an extra separation issue. In addition, it might be anticipated that the orthogonal fit between the two reaction steps might be better, as the photo-Claisen

* Authors for correspondence: v.hessel@tue.nl and and

DOI: 10.1556/1846.2016.00029

reaction is done at normal temperature so that (at least) the allyl bromide decomposition should be much reduced or even absent.

With such motivation on enlarged synthetic scope and improved orthogonality, we aim to develop a microflow protocol of the photo-Claisen rearrangement.

2. Results and Discussion

2.1. Parametric Sensitivities of the Photo-Claisen Rearrangement of Allyl Phenyl Ether in Microflow. It is known from the literature that the photo-Claisen rearrangement of allyl phenyl ether works well under given conditions in batch. Thus, we started our parametric investigation with the unsubstituted precursor (also because this molecule is commercially available, whereas we needed to synthesize the substituted molecules before the photo experiments).

2.1.1. Flow Process Development — Isomer Distribution/ Phenol Content and Conversion/Yield. In a typical batch experiment documented in the literature, the relative product distribution after the photoreaction of allyl phenyl ether is reported as 21% (ortho, 2-), 31% (para, 4-), and 48% (phenol) in hexane and 42% (ortho, 2-), 42% (para, 4-), and 16% (phenol) in MeOH (irradiation time = 4 h) [17]. Irradiation was conducted to about 30% conversion [17, 18]. In an own batch experiment, after 5 h of irradiation in 1-butanol (10 mL solution), no product was detected, while in photo microflow, we achieved 30% (ortho), 30% (para), and 21% (phenol) and, thus, could reach similar performance in batch mentioned above.

Five to seventy hours of irradiation time is quite common for batch-type photo Claisen experiments [18]. Therefore, in our batch experiments, we applied 5 h, while the photo microflow was most often finished in less than 8 min. This is due to the much smaller dimensions of the capillary providing a high transmittance throughout the reaction volume and, thus, ensuring high light efficiency. It is also beneficial to give a comparison of results for the different lamp wattages. Three more batch experiments, with different lamp power, found in the literature have been listed in Table 1. According to the results, it can be concluded that lamp with lower power gives lower conversion. For instance, the experiment with 10 W-low pressure mercury lamp gives 31.4% conversion in 24 h. On the other hand, the experiment with 15 W-low pressure mercury lamp gives higher conversion, 74% in 32 h. Although, in the second experiment, the reaction time increases by 25%, the conversion rises 2.3 times. It should be mentioned that the lamp power is not the only parameter which controls the conversion, yet it is one of the key parameters. Besides the lamp power, one should consider other parameter effects such as concentration, volume of the solution, and solvent. In this research, we aimed to use the low-power lamp and improve the other influential parameters instead. Also, Sugimoto et al. [21] has thoroughly studied the application of the Barton reaction in microreactors and the effect of different light sources. They showed that, in their case, an ultraviolet (UV)-LED lamp (1.7 W) is more efficient than a 300-W Hg lamp.

The photo microflow synthesis avoids the formation of migration of the double bound of the allyl group to give E/Z 2-(prop-1-enyl)phenols which were reported for the corresponding thermal (high-T) microflow synthesis of allyl phenyl ether, especially at temperatures above 300 °C [14]. These substances can undergo ring closure to give 3-dihydro-2-methylbenzo[b]furan and 2-methylbenzo[b]furan as further byproducts of the thermal process which we did not observe. The latter effect was remarkably dependent on the solvent in the thermal process, with alcoholic solvents giving the cleanest process.

2.1.2. Solvent Effect. One of the key parameters both for the thermal and photo-Claisen rearrangement is the selection of an appropriate solvent. Basic needs are to ensure that all reactants are soluble (which is particularly relevant for microflow synthesis), the solvent is transparent to the desired wavelength, and it should not suppress the photochemical process. We have already shown that, for the thermal Claisen microflow process variant, the performance varies largely with the solvent chosen. Even with the class of alcohols, considerable differences were found for diverse alkyl chain length, yet also even when comparing 1- and 2-alcohol isomers.

Since Hughes et al. [22] state that increasing polarity causes an increase in reaction rate for the photo-Claisen process, we would like to continue this investigation with alcohols as solvents of the choice. The explanation for the acceleration is that the transition state is more polar than the initial reagent so that it has more stabilization by interaction with the solvents. Besides polarity, hydrogen bond formation is responsible for the acceleration of the Claisen rearrangement [23–25]. Also, several other references give more evidence that polar solvents accelerate the Claisen rearrangement [26–28].

It is further known that the primary products of photo-Claisen rearrangement in protic (alcoholic) solvents are 2- and 4-allyl phenol, in almost comparable ratio, while 3-allyl phenol is formed in very small amount [29]. Thus, sufficient access to the desired para-product (4-allyl phenol) is given.

Table 2 shows that there is hardly any difference in the ultraviolet transmission (at diverse relevant wavelengths) and cut-off wavelengths of the majorly used alcohols. They have similar optical property as given for the nonpolar heptane solvent [30].

Figure 1 compares the yield of the photoflow product ortho-allyl phenol in methanol, 2-propanol, 1-butanol, and heptane. Later, we will comment on the formation of para-allyl phenol and phenol, yet here, the focus is on the ortho-product which is formed as largest fraction. It is evident that the alcohols as polar protic enhance the conversion as compared to the nonpolar heptane benchmark. This is in line with the observation that 1′,1′-dimethylallyl phenyl ether has a quantum yield of disappearance of 0.75 in i-propanol, whereas this value is 0.55 for cyclohexane [31]. Also, the conversion obtained by irradiation of diphenyl ether in methanol is 67%; however, the conversion drops significantly to 18% in *n*-hexane [34]. This effect has been justified in terms of stabilization of the intermediate cyclohexadienones by hydrogen bonding. Another possibility could be that the C–O cleavage in the excited singlet state is assisted by the presence of protic solvents [32].

Table 1. Comparison of the conversion of photo-Claisen rearrangement of allyl phenyl ether for different light source wattage in alcohol as solvent in batch system [18]

UV lamp	Time (h)	Solvent	Concentration (M)	Conversion (%)	Reference
10 W-low pressure mercury	24	2-Propanol	0.05	31.4	[19]
15 W-low pressure mercury	32	2-Propanol	0.03	74	[20]
450-medium pressure mercury	No time mentioned	Methanol	0.01	10–20	[1]
10 W-low pressure amalgam	5	1-Butanol	0.01	0	Our own experiment

Table 2. Ultraviolet transmission at diverse wavelengths and cut-off wavelengths of the majorly used alcohols and comparison to the nonpolar solvent heptane [30]

Solvent	%T 254 nm	%T 313 nm	%T 366 nm	T = 10% at λ (nm)
Heptane	100	100	100	197
Methanol	100	100	100	205
Ethanol	98	100	100	205
2-propanol	98	100	100	205

1-Butanol gives the best performance, followed by 2-propanol and methanol. The hydrogen bonding and polarity relate to the pK_a value [33, 34]. Yet, the reaction sequence does not follow the line of pK_a values: pK_a (methanol): 15.3, pK_a (2-propanol): 17.1, pK_a (1-butanol): 16.1, and, for comparison, pK_a (water): 15.7. Thus, the result is depending on other parameters as well.

Moreover, it can be clearly seen that 2 min is not long enough to ensure best yield under the given conditions. Rather, from 4 min onwards, a stable yield is achieved. Irradiation above 8 min leads to decrease in yield, probably by decomposition of the Claisen product to phenol. This happens already on a shorter time-scale for the heptane solvent. It was therefore concluded to perform most of the experiments reported here at the longest residence time which allowed for high yield, namely, 8 min. In this sense, it was aimed to ensure that also the less reactive substrates can show some yield under photoflow irradiation.

2.1.3. Concentration Effect. The concentration of reactants can have an impact on kinetics and overall productivity. In a photo process, an increase in the concentration of absorbing reactants decreases the radiation intensity. Also, photo-irradiation hardly penetrates deeper than 1 mm in a flask and provides a major argument to use microflow conditions throughout the capillary (100–1000 μm). This ensures that irradiation is present and can activate the photoreaction [35]. Due to this, microflow is able to operate under higher concentrations and, thus, has potential to achieve high space-time yields.

The radiation transport is a complicated process which is affected by the source of light, as well as the configuration of the photoreactor [36]. The Bouguer–Lambert–Beer equation (as shown in eq. 1) can be applied to single-phase (homogeneous) photochemical reactions.

$$T = \frac{I}{I_0} = 10^{-\varepsilon l c} \quad (1)$$

where ε is the molar extinction coefficient, c is the concentration of the absorbing species, and l is the light path length.

In order to achieve maximum transmittance, the distance between the lamp and capillary reactor was decreased as much as possible by winding the capillary around the cylindrical UV lamp. In this way, loss of irradiation through absorption in air was aimed to minimize. Major contributions in lowering UV transmittance through air are caused by the presence of water vapor, global warming gases, and dust particles. For this reason, vacuum UV has been established below ≈ 200 nm (far and extreme UV). The addition of water vapor (P_{H2O} = 8.5 mbar) to pure nitrogen leads to an increase in the absorption coefficient $\Delta\varepsilon \approx 0.56\times10^{-6}$ cm^{-1}, which almost doubles the absorption of dry air [37].

Figure 2 shows the yield obtained for diverse concentrations of allyl phenyl ether, ranging from 0.001 to 0.4.

It is evident that, up to a concentration of 0.05 M, good performance is achieved. Then, 10 min residence time is needed with the shorter times showing incomplete conversion. On the contrary, photoreaction at the lowest concentration is finished already after 2 min and longer residence times show reduced yield by photodegradation of the product. Operation at highest concentration (0.2 and 0.4 M) needs enlarged residence times and is incomplete in the time frame observed here.

The value of 0.05 M is near to what is commonly used for preparative photolysis. For example, 0.0625 M (500 mg of substrates in 56 mL of ethanol) meta-methoxyphenylallyl ether was converted in a preparative manner [38]. To ensure the light transmittance, petri dishes were used as flat reaction cells. Typical analytical photoreaction experiments are made at lower concentration, e.g., at 0.0001 M in water for the above given case [38]. Galindo reports use of concentrations from 0.01 M to 0.4 M in his photochemistry overview (Table A.1. in ref. [18]).

2.1.4. Distance from Light Source. The lamp used in the experiments reported here has a power of 10 W (providing a UV intensity of 21–24 microwatt/cm^2) This is at the lower edge of lamps used in the literature for UV photochemistry. Galindo reports in his overview the use of 6 W-lp-quartz to 450 W-mp lamps (lp: low pressure; mp: medium pressure) [18].

Even though it was absorbed above that, for the given low distance between reaction capillary and UV lamp, the energy of the UV light might be so high that it may cause degradation of the starting compound. This effect was noted at long residence time. Therefore, an experiment was made with increased distance between the capillary and the light source (see Figure 3) and, thus, allowing absorption of the UV light by air. Two-centimeter distance was given throughout the entire lamp perimeter.

The yield performance with 0 and 2 cm distance is very different, respectively. In case of tight contact, a decline of yield with residence time is observed for the given reason, whereas the reaction with capillary and lamp in a distance shows increasing yields. It is worth mentioning that the surface temperature of this UV lamp was measured after 30 min being in use and it did not exceed 35 °C. Therefore, adjusting the distance between capillary reactor and light source is a means to fine-tune the photo process.

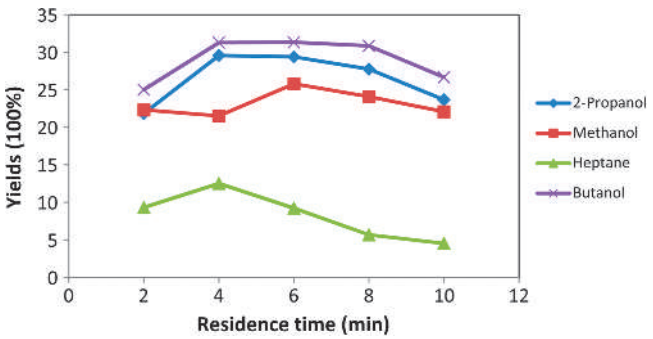

Figure 1. Yield of ortho-allyl phenol for some relevant alcoholic solvents and heptane (for comparison) versus residence time (at a concentration of 0.01 M allyl phenyl ether)

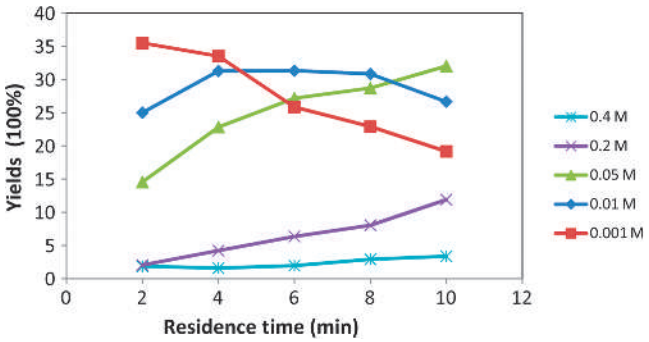

Figure 2. Yield of ortho-allyl phenol versus residence time for different concentration of allyl phenyl ether

2.2. Orthogonality — Process Simplification when Connecting to a Prior Nucleophilic Substitution. According to our previous research, when thermal-Claisen rearrangement was connected to nucleophilic substitution reaction in flow, the presence of allyl bromide and the base DBU used were negatively affecting the final product distributions and lowering considerably the product yield. This asks for continuous-flow separation which makes the process complex, as reported prior [12], and we aim here correspondingly for process simplification. Therefore, as described in the introduction, one of the goals of this work is to check the orthogonality when the photo-Claisen rearrangement is coupled with the nucleophilic substitution reaction. In order to study this, photo-Claisen rearrangement of allyl phenyl ether has been performed by manually adding allyl bromide and DBU, and the results are compared with the photo-Claisen rearrangement of allyl phenyl ether without any addition.

Figure 4 shows the resulting high-performance liquid chromatography (HPLC) chromatograms of the abovementioned experiments for the residence time of 6 min. As seen in Figure 4(a), the main products of photo-Claisen rearrangements are phenol, ortho, and para allyl phenol. Increasing the residence time may increase the possibility of secondary reactions or polymerization [11]. Thus, with the residence time higher than 6 min, some other byproducts could be formed.

Also, comparing Figure 4(a), (b), and (c), it can be seen that the presence of allyl bromide and DBU does not influence the photo-Claisen rearrangement; it does not lead to the formation of new products or affect product selectivity.

This result is fundamentally different to the respective HPLC chromatograms of thermal-Claisen rearrangement as reported in ref. [12]. In the thermal case, the product peak almost vanished and the chromatograms showed several new peaks due to the formation of side and decomposition products. Thus, the same reaction can be tuned orthogonal or non-orthogonal by choice of the activation mode.

2.3. Meta-Substituent Effect on Para to Ortho Isomer Distribution for the Photo-Claisen Rearrangement of Allyl Phenyl Ether in Microflow. White et al. [39] presented that electron-donating groups and polar solvents accelerate the reaction rate of the thermal Claisen rearrangement. The substituent effects are related to intramolecular forces while the solvation effects are correlated to intermolecular forces.

Pincock et al. [1, 40] reported also that substituent effects on the kinetic rates are significant and that the reaction rate of ethers with electron-donating groups (methoxy, methyl) is higher than ethers with electron-withdrawing groups (trifluoromethyl, cyano). The values are consistent with the change in bond dissociation energy relative to phenol which is $\sigma+$; ρ = +28.1 (r = 0.990) for ΔB_{DE} (kJ/mol) for both para- and meta-substituted compounds. This means that the bond is weakened by the electron-donating groups (ΔB_{DE}: −22 kJ/mol for 4-methoxy), while it is reinforced by the electron-withdrawing groups (ΔB_{DE}: +18 kJ/mol for 4-cyano). The reason behind this is not clearly mentioned; more precisely, there is an ambiguity as to which effect – changes in stability of the substituted phenols or changes in the stability of the substituted phenoxy radicals – is decisive. Although there is a controversy on this topic, the latest argumentations strongly support the latter factor. This effect may prevail over the other more typical substituent effects (electron density changes on excitation, resonance, induction, etc.) for the σ bond cleavage reactions of phenolic ethers because it is mostly large for XC6H4Y-Z cases when Y = O and Z = H or C. For other cases where Y = C and X = H, C, or halogen, the substituent has low influence on the BDE which seems to be ruled by the other effects of the substituent. The electron effects are found similar in MeOH and cyclohexane [31, 32].

The absolute differences in reactivity are huge and can span several orders of magnitude. For example, reaction rates measured in methanol for 4-OCH_3 and 4-CH_3 have been almost the same, being 530 and 510×10^7 (s^{-1}), respectively [1]. They are almost double as compared to the reaction rate of the unsubstituted molecule which was found to be 250×10^7 (s^{-1}). The latter still is more than 10 times ahead of a deactivated molecule (cyano group, 16×10^7 (s^{-1})). The use of different solvents can shift the relative sequence of reactivities, as, e.g., found when taking cyclohexane.

2.3.1. Substitution Effects in Photo Microflow. To investigate the above given effect for the photo-Claisen rearrangement in microflow, allyl aryl ethers with different relevant meta-substitution groups (X = H, CH_3, OCH_3, CF_3, and Cl) were synthesized from the corresponding phenols (see Scheme 1 and Table 3). This was achieved by reaction with allyl bromide

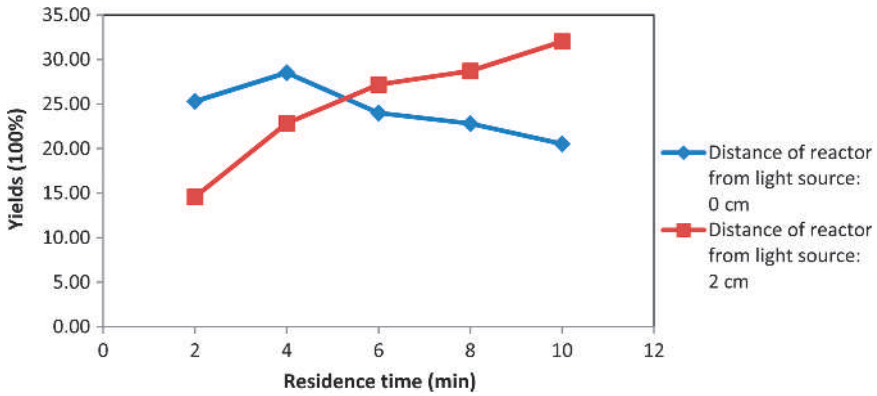

Figure 3. Yield of ortho-allyl phenol for 0.05 M allyl phenyl ether for two different distances of the reaction capillary from light source, being 0 cm and 2 cm

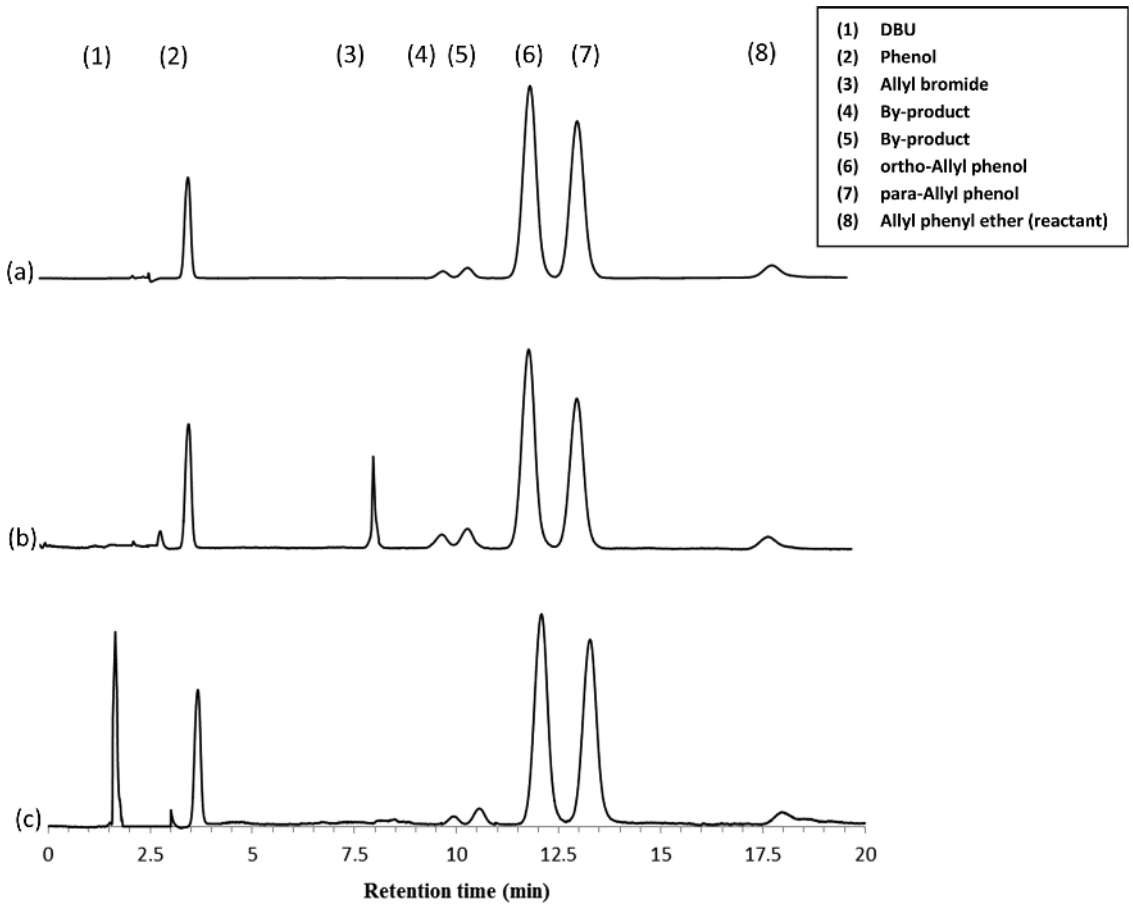

Figure 4. HPLC chromatograms of photo-Claisen rearrangement with 0.01 M allyl phenyl ether: (a) no additions, (b) with 1 eq. allyl bromide, and (c) with 1 eq. DBU (residence time = 6 min)

using potassium carbonate in dry acetone [40–43]. In line with the above given result for the parental compound with X = H and as expected from the literature, the major products for X = H, CH_3, OCH_3, and CF_3 are the corresponding phenols (2) and the rearranged allyl substituted phenols 2-allyl-3-X (4), 2-allyl-5-X (5), and 4-allyl-3-X (3) (see Table 3).

If we consider the yields given in Table 3 to qualitatively correlate to the rate constants (although this cannot be strict as probably an excess of residence time was given for some of the runs), it can be concluded that the photochemical Claisen rearrangement shows the same trend in substituent dependence as reported above for the thermal one. We therefore propose that changes in BDEs may have as well a major effect on the photochemical rate constants.

Scheme 1. Possible main products in the photo-Claisen rearrangement of 3-substituted allyl phenyl ethers in microflow

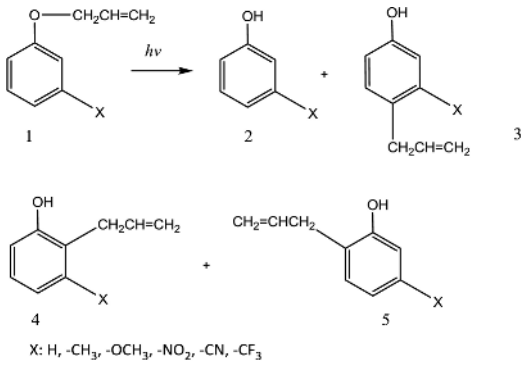

The 3-cyano and 3-nitro compounds are not listed in Table 3 because no product was formed in the "distant" reactor configuration (distance from light source = 2 cm) at 15 min residence time. However, in the "tight" process variant (distance from light source = 0 cm) and 100 min residence time, the 3-cyano compound reacted to give phenol (10%) as the main product and 9% of unknown products. According to the literature [1], 3-cyano compound is photochemically very unreactive and, even after the prolonged reaction time, some conversion happened but the product mixtures are very complicated and could not be characterized. Even under such forced conditions, the 3-nitro compound reacted not at all.

2.3.2. Substitution Effects in Photo Batch as Comparison. Table 4 shows the results of the respective batch experiments reported by Pincock et al. [1]. The total amount of all yields, which were obtained at low conversions (10–20%), were normalized to 100%. There is no report on the reaction time of these batch results, yet the first guess is that the batch residence time is much longer than the microflow reaction time. Also, since the batch results have been normalized, it is only possible to compare the product distribution in batch with the microflow results. Although there is no general trend, it seems that, in

Table 3. Product distribution (%100) for the photo-Claisen rearrangement of diverse 3-substituted allyl phenyl ethers at residence time = 8 min in microflow. Tight configuration (0 cm distance between the reaction capillary and the lamp)

Compound	Solvent	Product 2	Product 3	Product 4 + 5
X:H	1-Butanol	21	30	30
X:–CH_3	1-Butanol	15	35	42
X:–OCH_3	1-Butanol	13	19	53
X:–CF_3	1-Butanol	–	34	48

batch, the product distribution is higher for some of the 4-allyl and 5-allyl phenols and the phenol share is much lower in batch. This could be the case since these yields were taken at low conversions, and the results may change at higher conversions due to over-irradiation [18].

2.3.3. High-Temperature Photo Microflow. Photoreactions are known to heat up bigger vessels through their thermal radiation. Often, hazardous intermediates are accumulated in photoreactions such as singlet oxygen or peroxides. Therefore, the use of high temperatures is commonly not advised for safety reason. Microreactors allow the safe handling of even such conditions and, thus, to explore high-T photo microflow as novel process window.

There are reasons to do so. Schubnell et al. [44] explored the possibility of performing photochemistry at high temperature for the conversion of solar energy into chemicals using ZnO as solid photocatalyst. Temperature changes the photocharacteristics quite remarkably. The luminescence intensity decreases with increasing temperature because of vibrational level population which leads to a red shift of the spectra. The luminescence spectra also broaden with increasing temperature due to increased phonon populations. In the UV-photo synthesis of vitamin D_3, the provitamin 7-dehydrocholesterol is reacted via singlet state irradiation to the previtamin intermediate. By virtue of a temperature pathway, this is then transferred to vitamin D_3 [45], yet in competition with photo-induced equilibrium reactions to the side products tachysterol and lumisterol (which in turn can also be converted to vitamin D_3) [46, 47]. For our case, the Claisen rearrangement, motivation also might be that we simply like to omit the cooling-down step needed after the 100 °C hot nucleophilic substitution for reasons of process simplicity and energy efficiency. That might be especially desirable in case another high-temperature processing follows the Claisen rearrangement (making up a three-step flow synthesis). In a way, this means ensuring orthogonality in the combined process protocols.

Considering the above, and with the process window opened by our microreactor processing, the high-T photo microflow process variant of the Claisen rearrangement of allyl phenyl ether was investigated. The temperature could be set maximally to 78 °C, and that reaction performance was compared to room-temperature photo microflow operation (see Table 5). While the 3-meta 4-allyl phenol (product 3) is formed in a similar amount, the share of ortho products (3-meta 2-allyl phenol and 3-meta 6-allyl phenol; product 4 + 5) is much lower at the high temperature. The 3-meta phenol yield (product 2) is accordingly higher. Thus, the thermal pathway results in increased product degradation. A possible explanation could be that, by giving more energy in the form of thermal energy (in addition to the photo energy), the intersystem crossing takes place to create a triple radical pair, where the radical can escape from the solvent cage and generate more phenol.

It can be concluded that, while not finding better product-related performance, a still sufficient performance is given (which may be optimized), whenever other urgent issues (e.g., orthogonality-driven) would demand a high-temperature operation.

Table 4. Product distribution (%100) for the photo-Claisen rearrangement of diverse 3-substituted allyl phenyl ethers in batch. Please note that the given values are not yields, but yields normalized by the sum of all yields, i.e., the real yields will be much lower, as conversion was 10–20% [1]

Compound	Solvent	Product 2	Product 3	Product 4 + 5
X:H	Methanol	4	46	50
X:–CH_3	Methanol	8	25	68
X:–OCH_3	Methanol	8	40	52
X:–CF_3	Methanol	3	32	65

3. Conclusions

A microflow route was developed for the photo-Claisen rearrangement of allyl phenyl ether as parental compound and diverse 3-substituted allyl phenyl ethers. This was done with the vision to continue the continuous two-step microflow synthesis reported recently for the allyl-substitution of phenol followed by a thermal Claisen rearrangement [12]. Two measures reported here can contribute to increasing molecular diversity: first is the use of 3-substituted phenols as precursors and the second refers to the possibility to achieve the 4-allyl product, besides the two 2-allyl products. The latter (para-substitution) is unique to the photo pathway, whereas the thermal rearrangement is known to provide only ortho-pattern. Yet, in the photo pathway, the ortho products are formed as well and a share of the product is decomposed to the phenol starting material.

To give a complete process window view, some relevant parametric sensitivities could be tackled. The superiority of using alcoholic solvents could be shown, with 1-butanol being the best one. As shown before, by many other photo microflow processes, the reaction time could be dramatically reduced from several hours to 8 min and less. Moreover, it could be shown that operation at preparatively relevant high concentrations could be achieved. Yet, the offset in the given timeframe was at about 0.05 M. As third parameter, the distance between the reaction capillary and the UV lamp was varied, from tight contact (0 cm) to some distance (2 cm). In this way, the UV intensity can be adjusted to the reaction needs. For slow reactions and less reactive substrates, the tight contact mode can intensify the reaction (to higher conversion and conversion rates), while the distant mode allows to avoid an overdose of photons for reactive conditions and substrates. The latter can then decrease the undesired photodegradation. Finally, a high-temperature photo microflow process was investigated to combine two activation means and constitute a novel process window, enabled by microflow. Yet, this did not improve the reaction performance, but rather led to more photodegradation.

4. Reaction System and Methods

4.1. General Reagent Information. Allyl phenyl ether, 1-butanol, 2-propanol, methanol, heptane, 3-methoxyphenol, 3-methyl phenol, 3-cyanophenol, 3-nitrophenol, and 1,3-dinitrobenzene were purchased from Aldrich chemical company and used as received. For the flow experiment, solutions were prepared in volumetric flasks.

4.2. Experimental Section. In order to perform photo-Claisen rearrangement in flow, a microfluidic setup was assembled as shown in Figure 5. The photomicroreaction system consists of a capillary tube of 5 m length and 0.5 mm internal diameter (volume of ≈ 1 mL) which is made of fluorinated ethylene propylene (FEP 1548; Upchurch Scientific). This capillary is wound around a cylindrical UV light source placed inside a closed oven. The sample solutions were introduced in the photomicroreactor by using an HPLC pump (Knauer, Smartline 1050). Irradiation was carried out using a low-pressure amalgam lamp (TS23-212; Dinies Technologies GmbH). Directly after exiting the photomicroreactor, the product samples were collected into vials. The samples were

Table 5. High-T photo microflow process variant of the Claisen rearrangement of 3-methyl allyl phenyl ether ("tight" configuration) in 1-butanol, residence time = 8 min

	Product 2	Product 3	Product 4 + 5
Photo-Claisen at 20 °C	15	35	42
Photo-Claisen at 78 °C	29	34	29

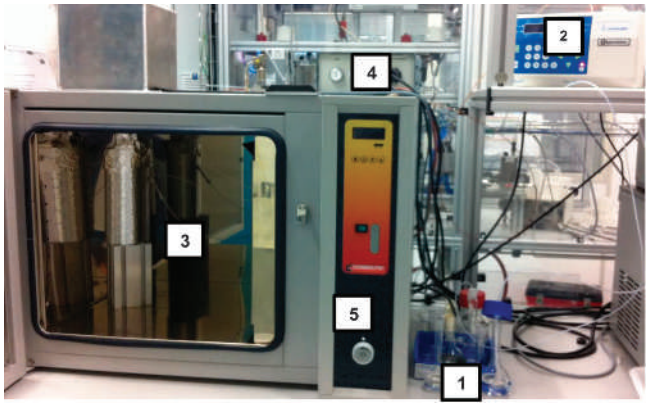

Figure 5. Microfluidic setup utilized for Claisen rearrangement. 1—Inlet and outlet of the microreactor; 2—HPLC pump; 3—light source surrounded with microreactor, covered with aluminum sheet; 4—light source power supply, 5—micro-photoreactor safety oven

analyzed with HPLC-UV for quantification by applying the internal standard method. Each data point in the plot constitutes the average of two samples.

The samples obtained from the photo-Claisen rearrangement of the 3-substituted allyl phenyl ether were analyzed with HPLC-UV. In order to identify the HPLC peaks, thermal-Claisen rearrangement of the same compounds was performed [12] and analyzed with HPLC-UV; also, one sample of the thermal-Claisen rearrangement of 3-methyl allyl phenyl ether was analyzed via nuclear magnetic resonance (NMR). Then, the thermal-Claisen results were compared with the photo-Claisen results. From the literature and the NMR results, it is known that the product of thermal Claisen rearrangement of 3-substituted allyl phenyl ether is 3-substituted 2-allyl phenol and 3-substituted 6-allyl phenol; product 4 + 5 [41]. By comparing the HPLC results of thermal-Claisen with photo-Claisen, the para product (3-substituted 4-allyl phenol) was also identified, along with the other two ortho products.

4.3. General Analysis Information. The samples were analyzed via ^{1}H NMR and HPLC. Nuclear magnetic resonance spectra were recorded on Varian 400 MHz or 500 MHz instruments. All ^{1}H NMR are reported in δ units, parts per million (ppm), and were measured relative to the signal for tetramethylsilane (0 ppm) in the deuterated solvent, unless otherwise stated.

HPLC analyses were performed on Shimadzu UFLC XR (205 nm) using a GraceSmart RP 18 5u column (150 mm, 4.2 mm). 1,3-Dinitrobenzene was used as an internal standard to carry out HPLC quantification in Claisen rearrangement of allyl phenyl ether.

4.4. Synthesis of 3-Substituted Allyl Phenyl Ethers. A mixture of one of the phenols (10 mmol), allyl bromide (12 mmol), and anhydrous K_2CO_3 (15 mmol) in dry acetone (20 mL) was refluxed under N_2 (reactions monitored by TLC). After completion of the reaction (10–20 h), the reaction mixture was cooled to room temperature and filtered through sintered funnel, and the filtrate was evaporated to remove the acetone. The residue was purified by column chromatography using petroleum ether–EtOAc as eluent to yield pure 3-substituted allyl phenyl ethers in an average yield of 90% [40–43].

3-Methyl allyl phenyl ether (1-allyloxy-3-methyl-benzene): ^{1}H NMR (400 MHz, $CDCl_3$) δ ppm 7.14 (t, ArH, 1H), 6.75 (dt, J = 8.0, 1.9 Hz, ArH, 1H), 6.72 (t, ArH, 1H), 6.70 (dt, J = 8.0, 1.9 Hz, ArH, 1H), 5.91–6.15 (m, CH=C, 1H), 5.40 (dq, J = 17.4, 1.6, 1.6, 1.8 Hz C=CH_2, 1H), 5.28 (dq, J = 10.6, 1.5, 1.5, 1.4 Hz, C=CH_2, 1H) , 4.51 (dt, J = 5.3, 1.5, 1.5 Hz, CH_2, 2H), 2.30(s, CH_3, 3H)

3-Methoxy allyl phenyl ether (1-allyloxy-3-methoxy-benzene): ^{1}H NMR (400 MHz, $CDCl_3$) δ ppm 7.15 (t, ArH, 1H), 6.45–6.64 (m, ArH, 3H), 5.92–6.18 (m, CH=C, 1H), 5.42 (dq, J = 17.4, 1.7, 1.7, 1.8 Hz C=CH_2, 1H), 5.29 (dq, J = 10.4, 1.5, 1.5, 1.4 Hz, C=CH_2, 1H), 4.52 (dt, J = 5.3, 1.5, 1.5 Hz, CH_2, 2H), 3.79 (s, CH_3, 3H)

3-Trifluoromethyl allyl phenyl ether (1-allyloxy-3-trifluoromethyl-benzene): ^{1}H NMR (400 MHz, $CDCl_3$) δ ppm 7.38 (t, ArH, 1H), 7.22 (d, J = 8.0 Hz, ArH, 1H), 7.16 (s, ArH, 1H), 7.09 (dd, J = 4.4, 8.1 Hz, ArH, 1H), 5.98–6.09 (m, CH=C), 5.44 (dq, J = 17.4, 1.6, 1.6, 1.8 Hz, C=CH_2, 1H), 5.32 (dq, J = 10.4, 1.5, 1.5, 1.4 Hz, C=CH_2, 1H), 4.60 (m, CH_2, 2H)

3-Nitroallyl phenyl ether (1-allyloxy-3-nitro-benzene): ^{1}H NMR (400 MHz, $CDCl_3$) δ ppm 7.78–7.81 (m, ArH, 1H), 7.75 (t, ArH, 1H), 7.43 (t, ArH, 1H), 7.25 (d, J = 16.5, Hz, ArH, 1H), 6.0–6.10 (m, CH=C), 5.45 (dd, J = 17.1, 1.4 Hz, C=CH_2, 1H), 5.35 (dd, J = 10.5, 1.2 Hz, C=CH_2, 1H), 4.63 (d, J = 5.5 Hz, CH_2, 2H)

3-Cyano allyl phenyl ether (1-allyloxy-3-cyano-benzene): ^{1}H NMR (400 MHz, $CDCl_3$) δ ppm 7.36 (t, ArH, 1H), 7.24 (dt, J = 7.6, 1.2, 1.2 Hz, ArH, 1H), 7.10–7.18 (m, ArH, 2H), 5.96–6.09 (m, CH=C, 1H), 5.42 (dq, J = 17.3, 1.6, 1.6, 1.5 Hz C=CH_2, 1H), 5.33 (dq, J = 10.6, 1.4, 1.4, 1.4 Hz, C=CH_2, 1H), 4.56 (dt, J = 5.2, 1.5, 1.5 Hz, CH_2, 2H)

2-Allyl-3-methylphenol and 2-allyl-5-methylphenol: ^{1}H NMR (500 MHz, $(CD_3)_2SO$) δ ppm 6.91 (d, J = 8.0 Hz, ArH, 1H), 6.89 (d, J = 7.7 Hz, ArH, 1H), 6.61 (d, J = 0.6 Hz, ArH, 1H), 6.6 (d, J = 8.1 Hz, ArH, 1H), 6.54 (d, J = 7.6 Hz, ArH, 2H), 6.51–6.56 (m, ArH, 1H), 5.88–6.02 (m, CH=C, 2H), 5.78–5.91 (m, CH=C, 2H), 4.85–5.06 (m, C=CH_2, 4H), 3.30–3.34 (m, CH_2, 2H), 3.29 (s, OH, 1H), 3.28 (s, OH, 1H), 3.23 (d, J = 6.7 Hz, CH_2, 2H), 2.19 (s, CH_3, 3H), 2.18 (s, CH_3, 3H)

Acknowledgment. We kindly acknowledge the European Research Council for the Advanced Grant on "Novel Process Windows—Boosted Micro Process Technology" No. 267443.

References

1. Pincock, A. L.; Pincock, J. A.; Stefanova, R. *J. Am. Chem. Soc.* **2002**, *124*, 9768–9778.
2. Hessel, V.; Kralisch, D.; Kockmann, N.; Noël, T.; Wang, Q. *ChemSusChem* **2013**, *6*, 746–789.
3. Smith, M. B.; March, J. *March's Advanced Organic Chemistry: Reactions, Mechanisms, and Structure,* edition 6; John Wiley and Sons, Inc.: Hoboken, New Jersey, 2006; vol. 9780471720.
4. Zelentsov, S.; Hessel, V.; Shahbazali, E.; Noël, T. *ChemBioEng Rev.* **2014**, *1*, 230–240.
5. Hessel, V.; Shahbazali, E.; Noël, T.; Zelentsov, S. *ChemBioEng Rev.* **2014**, *1*, 244–261.
6. Hessel, V.; Löwe, H. *Chem. Eng. Technol.* **2003**, *26*, 13–24.
7. Hessel, V.; Löwe, H. *Chem. Eng. Technol.* **2003**, *26*, 391–408.
8. Kobayashi, H.; Driessen, B.; van Osch, D. J. G. P.; Talla, A.; Ookawara, S.; Noël, T.; Hessel, V. *Tetrahedron* **2013**, *69*, 2885–2890.

9. Sato, M.; Otabe, N.; Tuji, T.; Matsushima, K.; Kawanami, H.; Chatterjee, M.; Yokoyama, T.; Ikushima, Y.; Suzuki, T. M. *Green Chem.* **2009**, *11*, 763.
10. Kong, L.; Lin, Q.; Lv, X.; Yang, Y.; Jia, Y.; Zhou, Y. *Green Chem.* **2009**, *11*, 1108–1111.
11. Maeda, H.; Nashihara, S.; Mukae, H.; Yoshimi, Y.; Mizuno, K. *Res. Chem. Intermed.* **2013**, *39*, 301–310.
12. Shahbazali, E.; Spapens, M.; Kobayashi, H.; Ookawara, S.; Noël, T.; Hessel, V. *Chem. Eng. J.* **2015**, *281*, 144–154.
13. Razzaq, T.; Kappe, C. O. *Chem. Asian J.* **2010**, *5*, 1274–1289.
14. Razzaq, T.; Glasnov, T. N.; Kappe, C. O. *Chem. Eng. Technol.* **2009**, *32*, 1702–1716.
15. Cambié, D.; Bottecchia, C.; Straathof, N. J. W.; Hessel, V.; Noël, T. *Chem. Rev.*, DOI: 10.1021/acs.chemrev.5b00707.
16. Knowles, J. P.; Elliott, L. D.; Booker-Milburn, K. I. *Beilstein J. Org. Chem.* **2012**, *8*, 2025–2052.
17. Pitchumani, K.; Warrier, M.; Ramamurthy, V. *J. Am. Chem. Soc.* **1996**, *118*, 9428–9429.
18. Galindo, F. *J. Photochem. Photobiol., C* **2005**, *6*, 123–138.
19. Koga, G.; Kikuchi, N.; Koga, N. *Bull. Chem. Soc. Jpn.* **1968**, *41*, 745–746.
20. Waespe, H. R.; Heimgartner, H.; Schmid, H.; Hansen, H. J.; Paul, H.; Fischer, H. *Helv. Chim. Acta* **1978**, *61*, 401–429.
21. Sugimoto, A.; Fukuyama, T.; Sumino, Y.; Takagi, M.; Ryu, I. *Tetrahedron* **2009**, *65*, 1593–1598.
22. Hughes, E. D.; Ingold, C. K. *J. Chem. Soc.* **1935**, 244.
23. Lee, A.; Stewart, J. D.; Clardy, J.; Ganem, B. *Chem. Biol.* **1995**, *2*, 195–203.
24. Uyeda, C.; Jacobsen, E. N. *J. Am. Chem. Soc.* **2008**, *130*, 9228–9229.
25. Huang, Y.; Unni, A. K.; Thadani, A. N.; Rawal, V. H. *Nature* **2003**, *424*, 146.
26. Lindsey, J. S.; Wagner, R. W. *J. Org. Chem.* **1989**, *54*, 828–836.
27. Severance, D. L.; Jorgensen, W. L. *J. Am. Chem. Soc.* **1992**, *114*, 10966–10968.
28. Davidson, M. M.; Hillier, I. H.; Hall, R. J.; Burton, N. A. *J. Am. Chem. Soc.* **1994**, *116*, 9294–9297.
29. Brandes, E.; Grieco, P. A.; Gajewski, J. J. *J. Org. Chem.* **1989**, *54*, 515–516.
30. Reichardt, C.; Welton, T. *Solvents and Solvent Effects in Organic Chemistry*, edition 4; Wiley-VCH Verlag GmbH & Co. KGaA: Weinheim, 2010.
31. Carroll, F. A.; Hammond, G. S. *J. Am. Chem. Soc.* **1972**, *94*, 7151–7152.
32. Haga, N.; Takayanagi, H. *J. Org. Chem.* **1996**, *61*, 735–745.
33. Ripin, D. H.; Evans, D. A. Pka table. http://evans.rc.fas.harvard.edu/pdf/evans_pKa_table.pdf (accessed November 04, 2005).
34. PKa, https://pubchem.ncbi.nlm.nih.gov/compound/1-butanol#section=Odor-Threshold (accessed September 16, 2004).
35. Coyle, E. E.; Oelgemöller, M. *Photochem. Photobiol. Sci.* **2008**, *7*, 1313.
36. Su, Y.; Straathof, N. J. W.; Hessel, V.; Noël, T. *Chem. – A Eur. J.* **2014**, *20*, 10562–10589.
37. Makogon, M. M.; Ponomarev, Y. N.; Tikhomirov, B. A. *Atmos. Ocean. Opt.* **2013**, *26*, 45–49.
38. Syamala, M. S.; Ramamurthy, V. *Tetrahedron* **1988**, *44*, 7223–7233.
39. White, W. N.; Wolfarth, E. F. *J. Org. Chem.* **1970**, *35*, 3585.
40. Gonzalez, C. M.; Pincock, J. A. *Can. J. Chem.* **2008**, *86*, 686–690.
41. Gozzo, F. C.; Fernandes, S. A.; Rodrigues, D. C.; Eberlin, M. N.; Marsaioli, A. J. *J. Org. Chem.* **2003**, *68*, 5493–5499.
42. Sayyed, I. A.; Thakur, V. V.; Nikalje, M. D.; Dewkar, G. K.; Kotkar, S. P.; Sudalai, A. *Tetrahedron* **2005**, *61*, 2831–2838.
43. Han, X.; Armstrong, D. W. *Org. Lett.* **2005**, *7*, 4205–4208.
44. Schubnell, M.; Kamber, I.; Beaud, P. *Appl. Phys. A* **1996**, *64*, 109–113.
45. Fuse, S.; Tanabe, N.; Yoshida, M.; Yoshida, H.; Doi, T.; Takahashi, T. *Chem. Commun.* **2010**, *46*, 8722–8724.
46. Gottfried, N.; Kaiser, W.; Braun, M.; Fuss, W.; Kompa, K. L. *Chem. Phys. Lett.* **1984**, *110*, 335–339.
47. Carey, F. A.; Sundberg, R. J. *Advanced Organic Chemistry Part A: Structure and Mechanisms,* Springer: New York, NY, 2007.